

# Edge effects in Bilayer Graphene Nanoribbons

Matheus P. Lima,<sup>1,\*</sup> A. Fazzio,<sup>1,2,†</sup> and Antônio J. R. da Silva<sup>1,‡</sup>

<sup>1</sup>*Instituto de Física, Universidade de São Paulo, CP 66318, 05315-970, São Paulo, SP, Brazil.*

<sup>2</sup>*Centro de Ciências Naturais e Humanas, Universidade Federal do ABC, Santo André, SP, Brazil*  
(Dated: May 29, 2018)

We show that the ground state of zigzag bilayer graphene nanoribbons is non-magnetic. It also possesses a finite gap, which has a non-monotonic dependence with the width as a consequence of the competition between bulk and strongly attractive edge interactions. All results were obtained using *ab initio* total energy density functional theory calculations with the inclusion of parametrized van der Waals interactions.

PACS numbers: 73.22.-f, 72.80.Rj, 61.48.De, 71.15.Nc

Since the synthesis of graphene[1], a plethora of intriguing properties has been found in this two dimensional zero gap crystal due to the presence of massless fermions with a high mobility[2, 3]. Besides the monolayer, stacking two layers of graphene still preserves the high mobility, and some features of the electronic spectrum can be controlled, for example, by applying an external electric field[4]. Measurements of quantum hall effect and quasi-particle band structure indicate qualitative differences between monolayers and bi-layers. The occurrence of this rich physics at room-temperature[5, 6] has attracted a great interest in designing graphene-based nanoelectronic devices. In this scenario, it is fundamental to establish and control an energy gap ( $E_g$ ).

A possibility is to introduce lateral quantum confinement via synthesis of single layer (GNR)[7, 8] or bilayer (B-GNR)[9, 10] graphene nanoribbons by plasma etching or chemical routes[11, 12]. This opens a gap that rises the possibilities to use graphene in nanoelectronics, where small widths (sub-10 nm) is required for room temperature applications[6]. However, the BGRNs are less sensitive to external perturbations in comparison with GNRs, and hence, they may be more appropriate to fabricate high quality nano-devices[13].

The electronic structure of the nanoribbons, including the gap, are largely affected by the geometric pattern (zigzag or armchair) at their edges. GNRs with zigzag edges, in particular, have as a distinct feature the presence of edge states that introduce a large density of states (DOS) at the Fermi energy. Theoretical works predict that this configuration is unstable, and there will be the appearance of a magnetic order that leads to a removal of this large DOS peak[7, 8, 14]. Magnetism in GNRs has been intensively investigated as a possible way to develop spintronic devices[15, 16, 17]. An anti-ferromagnetic (ferromagnetic) order between the two edges leads to a semiconductor (metallic) state[7, 8, 14]. It is also believed that magnetism is necessary to open a gap in zigzag B-GNR (B-ZGNR)[18].

In this Letter we investigate the geometrical and electronic structure of B-ZGNR, and show that the ground state of these systems is *non-magnetic and possesses a*

*non-monotonic finite gap*. There are two possible edge alignments for the B-ZGNR, called  $\alpha$  and  $\beta$  (see Fig. 1). We found that the  $\alpha$  alignment is energetically favorable, with an inter-layer edges attraction, whereas for the  $\beta$  alignment there is an inter-layer edges repulsion. These edge-related forces cause a deviation from the exact Bernal stacking, resulting in a non-monotonic behavior of the energy gap with the width  $w$  for the  $\alpha$  B-ZGNR, with a maximum value at  $w \approx 3.5nm$ . These results differ qualitatively from GNRs with zigzag edges (M-ZGNR)[11, 12]

All our results are based on *ab initio* total energy Density Functional Theory[19] (DFT) calculations. In order to correctly describe multi-layer graphitic compounds, it is necessary to include van der Waals (vdW) interactions. The use of fully relaxed total energy DFT calculations to study such systems suffers from serious limitations, since the most traditional exchange correlation ( $xc$ ) functionals in use today do not correctly describe these terms. With the LDA  $xc$ , the geometry is correctly described but the inter-layer binding energy is underestimated by

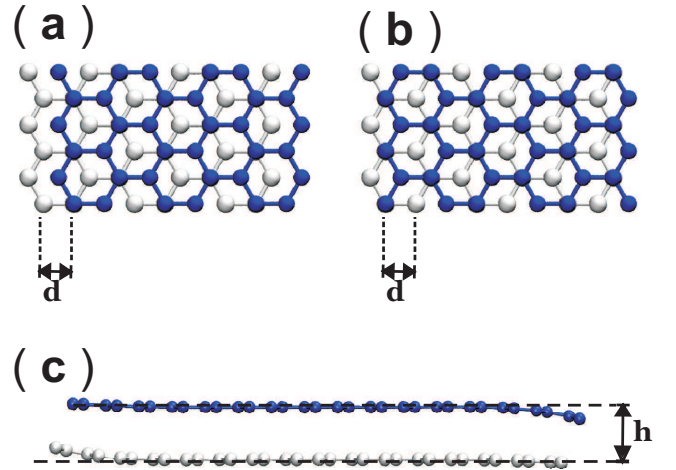


FIG. 1: Bilayer graphene nanoribbons with (a)  $\alpha$  and (b)  $\beta$  edge alignment. (c) Side view of bilayer graphene nanoribbons. The blue (white) atoms form the upper (bottom) layer.

TABLE I: Inter-layer binding energy ( $E_b$ ), in  $eV/atom$ , and distance  $h$ , in  $\text{\AA}$ , for graphite and a graphene bilayer, which is not bound (NB) at the GGA level.

|          |       | present | Exp                 | LDA   | GGA(PBE) |
|----------|-------|---------|---------------------|-------|----------|
| Graphite | $E_b$ | 0.054   | $0.052 \pm 0.005^a$ | 0.030 | 0.003    |
|          | $h$   | 3.350   | $3.356^b$           | 3.200 | 4.5      |
| Bilayer  | $E_b$ | 0.027   | -                   | 0.017 | NB       |
|          | $h$   | 3.320   | -                   | 3.202 | NB       |

<sup>a</sup>From Ref. [21]

<sup>b</sup>From Ref. [22]

50%, whereas the GGAs  $xc$  do not even correctly describe the geometrical features[20]. Thus, in order to be able to investigate the geometries and relative energies of B-ZGNRs, we include a non-local potential in the Kohn-Sham (KS) equations that correctly describes the vdW interactions. We modified the SIESTA code[23] adding in the KS Hamiltonian[24] the dispersion corrected atom centered potential (DCACP)[25]. This correction is sufficiently accurate to describe weakly bonded systems[26] with the vdW interactions included in the whole self-consistent cycle, providing accurate values for both forces (and thus geometries) and total energies. Our implementation was successfully tested (see Table I), and was employed to obtain the results here reported[28, 29, 30].

We investigated B-ZGNR composed by two M-ZGNR passivated with hydrogen, and widths[31] that range from  $w = 0.6$  to  $w = 4.5$  nm. The layers are in the Bernal stacking, which means that there are two types of C atoms, those that are positioned above the center of the hexagons of the other layer, defining a B-sublattice, and those right on top of the C atoms of the other layer, forming an A-sublattice. An infinite graphene bilayer has no gap, and the orbitals at the Fermi level are located at the B-sublattice. When we cut the layer along the zigzag edge, there are two possible alignments (Fig.1): (a) the  $\alpha$  alignment, where the outermost edge atoms belong to the A-sublattice, and (b) the  $\beta$  alignment, where the outermost edge atoms belong to the B-sublattice. Thus, only the inter-layer edge interaction differs. Two geometrical distortions have proven to be important: (i) an edge distortion that causes a curvature in the ribbons (see Fig.1(c)), and (ii) a lateral deviation from the perfect Bernal stacking. To quantify this deviation, we define the quantity  $u \equiv d_{C-C} - d$ , where  $d$  is shown in Fig.1(a) and (b), and  $d_{C-C}$  is the carbon-carbon bond length. The perfect Bernal stacking corresponds to  $u = 0$ .

The geometries and band structures of fully relaxed B-ZGNRs with  $w \approx 1.0$  nm for  $\alpha$  and  $\beta$  alignments are presented in Fig. 2. In B-ZGNR with the  $\beta$  alignment, similarly to M-ZGNRs, a non spin-polarized calculations leads to a high DOS at the Fermi energy, and a magnetic

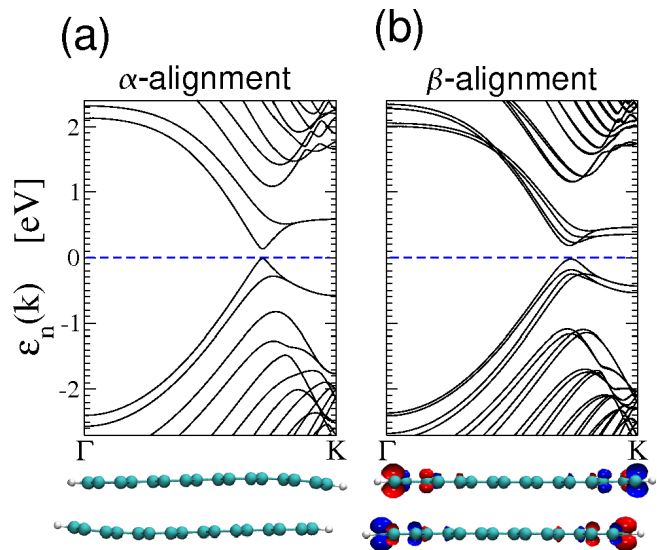


FIG. 2: Ground State of fully relaxed B-ZGNRs generated by stacking two (5,0) M-ZGNR. Below each band structure the geometry and local magnetization are presented. (a)  $\alpha$  alignment. This state is non-magnetic and presents a geometric distortion near the edge. (b)  $\beta$  alignment. This state shows an AF in-layer and AF inter-layer magnetic order.

order is required to split these localized edge states at the  $K$  symmetry point. In order to establish the possible spin polarized configurations, we used four initial guesses for the density matrix before starting the self-consistency cycle, which are: *i*) anti-ferromagnetic (AF) in-layer and inter-layer, *ii*) ferromagnetic (F) in-layer and inter-layer, *iii*) AF in-layer and F inter-layer and *iv*) F in-layer and AF inter-layer. As well as non-polarized calculations. From all calculations, the AF in-layer and inter-layer guess leads to the lower energy state (Fig. 2(b)). However, the energy differences are less than  $k_B T$ [18].

At the  $\alpha$  alignment (Fig. 2(a)), on the other hand, we obtain a qualitatively new situation. There is a strong attractive interaction between the edge atoms of the two layers, with a resulting geometric distortion that decreases the distance between them (Fig. 2(a)). For all  $\alpha$  B-ZGNRs that we have investigated, the final geometry always had an inter-layer edge atoms distance around 3.0  $\text{\AA}$ . The final configuration is non-magnetic and with a finite gap, contrary to previous results where the presence of a gap was intrinsically coupled to a magnetic state[18]. Note that if we do not allow the atoms at the two layers to relax, but simply optimize the inter-layer distance (*i.e.*, the layers keep their planar geometries), a magnetic configuration is still necessary to open a gap[18]. However, this configuration has higher energy.

If we take one of the mono-layers that form the final relaxed  $\alpha$  B-ZGNR, and perform a calculation without letting the atoms relax, we obtain an energy increase, when compared to the lowest energy M-ZGNR (AF in-layer[15]), that can be broken down in two components.

Considering M-ZGNR with widths larger than 2 nm, if we allow the distorted monolayer to be magnetic, the energy increase is  $\approx 0.1$  eV/nm, which can be viewed as the elastic contribution. If we now consider a non-magnetic configuration for this distorted monolayer, which is the situation in the  $\alpha$  B-ZGNR, there is an extra energy increase of  $\approx 0.4$  eV/nm, *i.e.*, an overall energy penalty of  $\approx 0.5$  eV/nm. Considering the two monolayers, the total energy cost to deform and demagnetize the  $\alpha$  B-ZGNR is  $\approx 0.96$  eV/nm. This energy increase is more than compensated by the edge atoms interaction, and the energy gain is in part associated with a large split of the localized edge states. At the  $\beta$  B-ZGNR (Fig. 2(b)), the unique way to diminish the DOS associated with the localized edge states at the Fermi energy is via a magnetic ordering, and the system tends to increase the inter-layer edge atoms distance in order to allow a bigger magnetization, given rise to a repulsive inter-layer edge interaction.

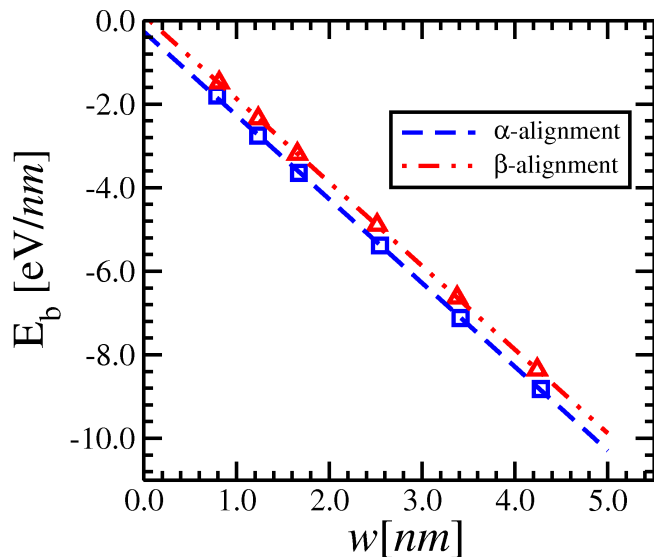


FIG. 3: Dependence of the binding energies with the width.

Comparing the two alignments, the  $\alpha$  B-ZGNR results energetically favorable. This is an even more important conclusion considering that most of the calculations used the  $\beta$  B-ZGNR[10, 32]. Fig. 3 presents the dependence of the B-ZGNRs binding energies, for both edge alignments, as a function of  $w$  (calculated relative to two isolated lowest energy M-ZGNR). The interaction between the layers can be separated into two components: *i*) edge interactions, that do not depends on the width, *ii*) and bulk interactions, that increase linearly with  $w$ . The binding energies (per unit length) can be well adjusted with:

$$E_b(w) = a + bw. \quad (1)$$

Since there are two edges,  $a/2$  is the inter-layer edge interaction energy per unit length, and  $b$  is the inter-layer bulk interaction energy per unit area. At the  $\alpha$  alignment,  $a = -0.26$  eV/nm and  $b = -2.0$  eV/nm<sup>2</sup>, indicating

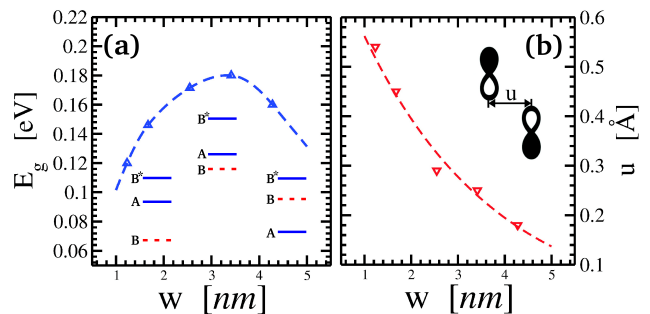


FIG. 4: Dependence of the (a) energy gap (inset illustrates the change of character of the VBM), and (b) the lateral deviation  $u$  with the width  $w$  (inset indicates how  $u$  affects the inter-layer A-sublattice  $p$ -orbitals interaction).

that the edges interaction is attractive ( $a < 0$ ). For the  $\beta$  alignment,  $a = +0.13$  eV/nm and  $b = -2.0$  eV/nm<sup>2</sup>, indicating that there is a repulsive edges interaction ( $a > 0$ ), showing that its stability results solely from the bulk. The parameter  $b$ , as expected, does not depend on the edge alignment, and it is very close to our calculated bulk inter-layer interaction in a graphene bilayer ( $0.027$  eV/atom =  $-1.99$  eV/nm<sup>2</sup>).

For the  $\alpha$  B-ZGNR, there is a competition between the forces deriving from the bulk, that do prefer the Bernal pattern of stacking, and the forces deriving from the edges, that tend to maintain the inter-layer edge carbon atoms distance close to 3 Å. The system then minimizes the overall energy penalty by simultaneously optimizing both the deviation  $u$  from the exact Bernal stacking, and the elastic energy associated with the ribbon's curvature. Thus, for narrower B-ZGNR the system prefers to have a larger value of  $u$  and a smaller overall curvature whereas for wider B-ZGNR the deviation  $u$  tends to decrease to minimize the bulk energy penalty, since now it is possible to have a softer curvature that is somewhat localized at the edges when compared to the total width of the ribbon (see Fig. 1(c)). As a result, the dependence of the lateral deviation  $u$  with the width  $w$  is well adjusted by  $u(w) = 0.80e^{-0.35w}$  (with  $u$  in [Å], and  $w$  in [nm]). Moreover, as a result, the carbon-carbon bond lengths do not significantly differ from their values in the M-ZGNRs. For this situation, the average inter-layer distance  $h$  is close to its value in the graphene bilayer (see Tab. I).

Without the geometrical deformation caused by the inter-layer edge interactions, a monotonic decrease of the energy gap is expected due to the quantum confinement ( $\propto 1/w$ )[8, 18]. However, for small ribbons, we find that the character of the valence band maximum (VBM) is located at the A-sublattice, as opposed to larger ribbons where it is located in the B-sublattice (see Fig. 4(a)), similarly to the Fermi level orbitals in the infinite graphene bilayer. Moreover, since the interaction between the C atoms in the A-sublattice increases when

$u$  decreases (see Fig.4(b)), the gap initially increases with  $w$ . However, for  $w \gtrsim 3.5 \text{ nm}$ , due to the quantum-confinement decrease, there is a crossover between the two highest occupied bands, and the character of the VBM is at the B-sublattice. Thus, this leads to a non-monotonic behavior of the energy gap with  $w$  (Fig. 4(a)).

For the  $\beta$  B-ZGNR, there is a repulsive interaction between the edges, in such way that the inter-layer edge carbon atoms distance is close to  $3.7 \text{ \AA}$ . There happens a small negative lateral deviation ( $u < 0$ ) that can be neglected when  $w > 1.6 \text{ nm}$ . Note that for the  $\alpha$  B-ZGNR, due to the attractive edges interaction,  $u > 0$ . We also found that, despite the presence of a magnetic order, the energy gap disappears when  $w > 3 \text{ nm}$ .

Summarizing, we unequivocally show that for B-ZGNR the edge alignment  $\alpha$  is the lowest energy configuration. This is a result of the strong attractive interaction between the edges, that is manifested in an observed chemical bonding between the inter-layer edge carbon atoms, and that significantly influences the geometry and electronic structure of bilayer nanoribbons with *sub-10 nm* widths. As a consequence, the ground-state is non-magnetic and possesses a finite gap, which presents a non-monotonic dependence with the width.

We acknowledge helpful discussions with M. D. Coutinho-Neto regarding the DCACP, financial support from FAPESP and CNPq.

---

\* mplima@if.usp.br

† fazzio@if.usp.br

‡ ajrsilva@if.usp.br

- [1] K. S. Novoselov, A. K. Geim, S. V. Morozov, D. Jiang, Y. Zhang, S. V. Dubonos, I. V. Grigorieva, and A. A. Firsov, *Science* **306**, 366 (2004).
- [2] K. S. Novoselov, Z. Jiang, Y. Zhang, S. V. Morozov, H. L. Stormer, U. Zeitler, J. C. Maan, G. S. Boebinger, P. Kim and A. K. Geim, *Nature* **438**, 197 (2005); Y. B. Zhang, Y. W. Tan, H. L. Stormer, P. Kim, *Nature* **438**, 201 (2005).
- [3] A. H. Castro Neto, F. Guinea, N. M. R. Peres, K. S. Novoselov, and A. K. Geim, *Rev. Mod. Phys.*, accepted.
- [4] K. S. Novoselov, E. McCann, S. V. Morozov, V. I. Fal'ko, M. I. Katsnelson, U. Zeitler, D. Jiang, F. Schedin, A. K. Geim, *Nat. Phys.* **2**, 177 (2006); T. Ohta, A. Bostwick, T. Seyller, K. Horn, E. Rotenberg, *Science* **313**, 951 (2006); J. B. Oostinga, H. B. Heersche, X. L. Liu, A. F. Morpurgo, L. M. K. Vandersypen, *Nat. Mat.* **7**, 151 (2008).
- [5] K. S. Novoselov, Z. Jiang, Y. Zhang, S. V. Morozov, H. L. Stormer, U. Zeitler, J. C. Maan, G. S. Boebinger, P. Kim, A. K. Geim, *Science* **315**, 1379 (2007); N. Tombros, C. Jozsa, M. Popinciuc, H. T. Jonkman, B. J. van Wees, *Nature* **448**, 571 (2007).
- [6] X. R. Wang, Y. J. Ouyang, X. L. Li, H. L. Wang, J. Guo, H. J. Dai, *Phys. Rev. Lett.* **100**, 206803 (2008).
- [7] Y. W. Son, M. L. Cohen, S. G. Louie, *Phys. Rev. Lett.* **97**, 216803 (2006).
- [8] L. Yang, C. H. Park, Y. W. Son, M. L. Cohen, S. G. Louie, *Phys. Rev. Lett.* **99**, 186801 (2007).
- [9] K.-T. Lam and G. Liang, *Appl. Phys. Lett.* **92**, 223106 (2008).
- [10] E. V. Castro, N. M. R. Peres, and J. M. B. Lopes dos Santos, *JOAM* **10**, 1716 (2008).
- [11] M. Y. Han, B. Ozyilmaz, Y. B. Zhang, P. Kim, *Phys. Rev. Lett.* **98**, 206805 (2007).
- [12] X. L. Li, X. R. Wang, L. Zhang, S. W. Lee, H. J. Dai, *Science* **319**, 1229 (2008).
- [13] Y. M. Lin, P. Avouris, *Nano Lett.* **8**, 2119 (2008).
- [14] L. Pisani, J. A. Chan, B. Montanari, and N. M. Harrison, *Phys. Rev. B* **75**, 064418 (2007).
- [15] T. B. Martins, R. H. Miwa, A. J. R. da Silva, A. Fazzio, *Phys. Rev. Lett.* **98**, 196803 (2007).
- [16] Y. W. Son, M. L. Cohen, S. G. Louie, *Nature* **444**, 347 (2006)
- [17] E. J. Kan, Z. Y. Li, J. L. Yang, J. G. Hou, *J. Am. Chem. Soc.* **130**, 4224 (2008)
- [18] B. Sahu, H. Min, A. H. MacDonald, S. K. Banerjee, *Phys. Rev. B* **78**, 045404 (2008).
- [19] P. Hohenberg, W. Kohn, *Phys. Rev.* **136**, B864 (1964); W. Kohn and L.J. Sham, *Phys. Rev.* **140**, A133 (1965).
- [20] M. Hasegawa, K. Nishidate, H. Iyetomi, *Phys. Rev. B* **76**, 115424 (2007) and references therein.
- [21] R. Zacharia, , H. Ulbricht, T. Hertel, *Phys. Rev. B* **69**, 155406 (2004)
- [22] A. Bosak, M. Krisch, M. Mohr, J. Maultzsch, C. Thomsen, *Phys. Rev. B* **75**, 153408 (2007)
- [23] E. Artacho, D. Sanchez-Portal, P. Ordejon, A. Garcia, J. M. Soler, *Phys. Status Solidi B* **215**, 809 (1999).
- [24] The added matrix elements are  $H_{\mu\nu}^{DCACP} = \sum_j \sum_{m=-l}^l \langle \varphi_\mu p_j^{lm} \rangle \sigma_j^1 \langle p_j^{lm} \varphi_\nu \rangle$ , where  $\{\varphi_\mu\}$  are the localized basis. We use only  $l=3$ , and centered at each atom  $j$  there is a normalized projector  $p_j^{lm}(\mathbf{r}) \propto Y_{lm}(\hat{\mathbf{r}}) r^l \exp\left(-\frac{r^2}{2\sigma_2^2}\right)$ , where  $Y_{lm}$  are spherical harmonics. The parameters  $(\sigma_1, \sigma_2)$  are from Ref. [27].
- [25] O. A. von Lilienfeld, I. Tavernelli, U. Rothlisberger, D. Sebastiani, *Phys. Rev. Lett* **93**, 153004 (2004).
- [26] E. Tapavicz, I. C. Lin, O. A. von Lilienfeld, I. Tavernelli, M. D. Coutinho-Neto, U. Rothlisberger, *J. Chem. Theory Comput.* **3**, 1673 (2007); O. A. von Lilienfeld, I. Tavernelli, U. Rothlisberger, D. Sebastiani, *Phys. Rev. B* **71**, 195119 (2005)
- [27] I. C. Lin, M. D. Coutinho-Neto, C. Felsenheimer, O. A. von Lilienfeld, I. Tavernelli, U. Rothlisberger, *Phys. Rev. B* **75**, 205131 (2007).
- [28] We use a generalized gradient approximation[29], norm-conserving pseudopotentials[30], a mesh cut off of  $400Ry$  for the grid integration, a  $1 \times 1 \times 50$  mesh for the first Brillouin zone sampling, a force criterion of  $10meV/\text{\AA}$ , and a supercell approximation with a lateral separation between the images of  $20\text{\AA}$ .
- [29] J. P. Perdew, K. Burke, M. Ernzerhof, *Phys. Rev. Lett.* **77**, 3865 (1996).
- [30] N. Troullier and J. L. Martins, *Phys. Rev. B* **43**, 1993 (1991).
- [31] We have defined the width as the lateral distance between the outermost C edge atoms of the bilayer.
- [32] E. V. Castro, N. M. R. Peres, J. M. B. Lopes dos Santos, A. H. Castro Neto, F. Guinea, *Phys. Rev. Lett.* **100**, 026802 (2008). J. Rhim, K. Moon, *J. Phys. Condens. Matter*, **20**, 365202 (2008).